Journal of Instrumentation

Quality control of mass production of PMT modules for DAMPE

To cite this article: J.N. Dong *et al* 2017 *JINST* **12** T05004

JINST

PUBLISHED BY IOP PUBLISHING FOR SISSA MEDIALAB

RECEIVED: *February 7, 2017*
REVISED: *April 23, 2017*
ACCEPTED: *May 12, 2017*
PUBLISHED: *May 26, 2017*

TECHNICAL REPORT

Quality control of mass production of PMT modules for DAMPE

J.N. Dong,[a,c] **Y.L. Zhang,**[a,b,1] **Z.Y. Zhang,**[a,b] **Y.F. Wei,**[a,b] **L.B. Wu,**[a,b] **C. Wang,**[a,b] **Z.T. Shen,**[a,b] **C.Q. Feng,**[a,b] **S.S. Gao,**[a,b] **F.J. Gan,**[a] **S.C. Wen,**[d] **Y.M. Hu,**[d] **D.Y. Chen,**[d] **Y.Z. Gong,**[d] **H.S. Huang,**[a,b] **X.L. Wang,**[a,b] **Z.Z. Xu,**[a,b] **S.B. Liu**[a,b] **and Q. An**[a,b]

[a] *State Key Laboratory of Particle Detection and Electronics, University of Science and Technology of China, Hefei, Anhui 230026, China*
[b] *Department of Modern Physics, University of Science and Technology of China, Hefei, Anhui 230026, China*
[c] *Department of Physics, University of Science and Technology of China, Hefei, Anhui 230026, China*
[d] *Purple Mountain Observatory, Chinese Academy of Science, Nanjing, Jiangsu 210008, China*

E-mail: ylzhang@ustc.edu.cn

ABSTRACT: Photomultiplier tube (PMT) modules were selected to read out the signals in the BGO electromagnetic calorimeter for the Dark Matter Particle Explorer satellite. The test procedure and the related quality control of mass production PMT modules are described, with a summary of PMT module quality and the results from tests. With strict quality control throughout the production and test process, over 88% of the PMT modules meet the criteria required by DAMPE.

KEYWORDS: Calorimeters; Gamma telescopes; Large detector systems for particle and astroparticle physics

[1] Corresponding author.

doi:10.1088/1748-0221/12/05/T05004

2017 JINST 12 T05004

Contents

1 Introduction

The Dark Matter Particle Explorer (DAMPE) satellite [1, 2] has been operating in space since December 17, 2015, and considerable science data have already been obtained. The BGO electromagnetic calorimeter (BGO ECAL) is the key sub-detector of DAMPE for measuring electrons, positrons and gamma rays of energies up to 10 TeV [3, 4]. The day-by-day calibrations show that all 1848 readout channels from 616 PMT modules perform properly. The successful operation of the BGO ECAL can be attributed to the strict quality control of PMT modules during mass production. In the following sections, we describe the BGO ECAL, and the quality control of mass production PMT modules. Our conclusions are presented in the last section.

2 BGO ECAL

The BGO ECAL is the most critical sub-detector for measuring electrons, positrons and gamma rays of energies from 5 GeV to 10 TeV [5]. It is composed of 308 BGO crystal bars with a size of $2.5 \times 2.5 \times 60\,\mathrm{cm}^3$. Each BGO crystal bar is viewed by two PMT modules from both sides, respectively.

The BGO ECAL must operate over a high dynamic energy range. The maximum deposited energy in one BGO bar is expected to be $\sim$ 2 TeV for a 10 TeV electron shower, according to a Monte Carlo simulation. In contrast, the energy calibration of the BGO ECAL relies on minimum ionizing particles (MIPs). The deposited energy from a minimum ionizing particle (MIP) passing through the 2.5 cm thick BGO bar is $\sim$ 23 MeV. To efficiently discriminate between electron and proton shower profiles, which is critical for hadron background rejection, a lower energy measurement of < 0.5 MIPs is needed. This corresponds to a range of energies from 11 MeV (~ 0.5 MIPs) to 2 TeV. The readout from each BGO bar must therefore cover a dynamic range of $\sim 2 \times 10^5$. To ensure the proper measurement of energies down to 11 MeV, the BGO light signals are attenuated to provide $\sim$ 100 fC per MIP from dynode 8 of the PMT. This provides a dynamic range on dynode 8 for energy measurement from 0.5 MIPs to $\sim$ 100 MIPs, a factor of 200. To provide the necessary charge output, the PMT amplification from dynode 2 to dynode 8 must be at least a factor of 1000 [6, 7].

A total of 616 PMT modules are needed to read out the 308 BGO crystal bars in the BGO ECAL. In order to ensure that a sufficient number of PMTs met the performance targets, 880 PMTs were purchased and 800 PMT modules were assembled. The detailed mass production and quality control (QC) are described in the next section.

3 Quality control of the PMT Modules during mass production

3.1 PMT module design

The structure of a PMT module is shown in figure 1. The PMT is an R5610A-01 (Hamamatsu) phototube with 10 dynode stages [8]. Three dynodes (dynodes 2, 5, and 8) are read out through a PMT baseboard [7]. The relative gain, from the second dynode to the eighth dynode, is required to be > 1000, with good linearity under normal high voltage.

The PMT is wrapped with two layers of amorphous alloy strips, to provide good magnetic shielding [9], and is inserted and glued into an aluminum sleeve. The sleeve provides mechanical protection for the tube. The sleeve and the black glue protect the PMT from external light.

The PMT is soldered to the baseboards before the PMT module is completed by connecting two aluminum T-shaped support pieces and a polyimide bracket. These are used to fix the PMT module to the lattice of BGO bars.

The PMT modules produced in this way have the advantage of magnetic and optical shielding and are less likely to be damaged. This greatly improves the ease and efficiency of installation.

3.2 Quality control for PMT selection

Before beginning PMT module production, it is of great importance to choose the proper PMTs. One way to obtain the most suitable PMTs is to require the manufacturer to choose high-performance PMTs meeting the requirements. However, because of budgetary constraints, we opted to select the proper PMTs by ourselves and design and manufacture our own test system.

88 PMTs at a time were placed in a dark box and powered continuously (1000V, $\sim$ 100 hours). The dark counts of the PMTs were tested and recorded every 20 hours. Those with dark count rates < 10 Hz were considered to be qualified.

Out of the 880 purchased PMTs, 828 were selected and 800 were inserted into PMT modules.

3.3 Quality control for PMT module assembly

During the mass production of the PMT modules, we used a set of documents to guide the assembly procedure and quality control to ensure good quality of production and to minimize the expenditure.

2017 JINST 12 T05004

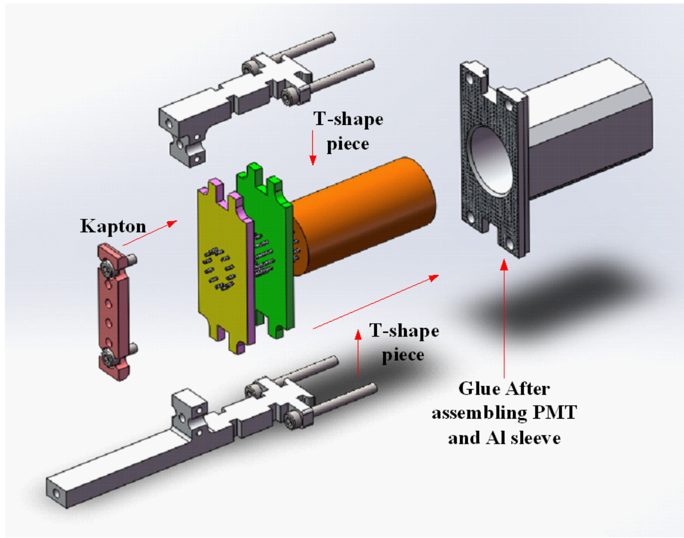

Figure 1. Structure of the PMT module.

These documents included a step-by-step PMT module production manual, a flow diagram of quality control, manufacturer cards, check cards, and record tables for test results.

Figure 2 shows the flow chart of PMT module production procedure. There are five check points in total.

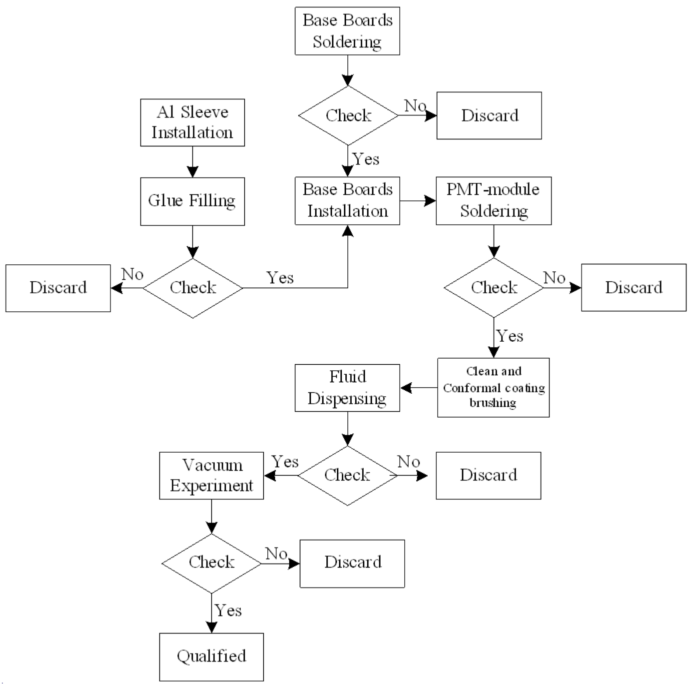

Figure 2. Flowchart of the production procedure for PMT modules.

First, the PMT was inserted inside the aluminum sleeve and fixed in position by pouring in a fast curing black glue (silicone elastomer kit , SYLGARD 170 [10]), at low pressure (~ 1 mbar).

2017 JINST 12 T05004

In this process bubbles were not allowed, in order to prevent any risk that the glue might explode in the vacuum in space. The definitive processing technology and work flow were confirmed after repeated trials. By examining the test glue stick in each filling batch, batches with no bubbles were qualified while those with bubbles were discarded. A photograph of a typical qualified PMT module, glued inside its aluminum sleeve, is shown in figure 3(a). In addition, attention also had to be paid to the status of the gelled glue. A typical below grade example is shown in figure 3(b), which shows that the glue blocks part of the entrance window of the PMT.

Second, the baseboards were prepared. Components were soldered to the baseboards in compliance with aerospace quality control regulations [11]. If their electrical performance is good, a thermal stress screening test can be performed [12], in which case the baseboards were put into an incubator. The temperature was cycled from $-45\,^{\circ}\mathrm{C}$ to $+75\,^{\circ}\mathrm{C}$ and it was held for 1.5 hours at the highest point and for 2 hours at the lowest point in every cycle. During this process, baseboards that passed all of the electrical tests such as capacitance and resistance tests were considered to be qualified.

Third, the qualified baseboards were assembled and the PMTs were soldered in their proper positions. If the module passed the electrical test, then it was cleaned and brushed with a conformal coating. A fluid (GD414, a silicon rubber made in China, used in the aerospace industry [13]) was dispensed near the soldered joints of the cables to maintain the electrical properties of the system. The PMT module was deemed qualified if it passed a wire guide test, a cable continuity test and a detailed visual inspection to assess the quality of the assembly.

Finally, the PMT module was put into a vacuum tank and powered with high voltage at 900V for ~ 4 hours. If there were no breakdown phenomenon, the PMT module was considered qualified. A photograph of a typical finished product is shown in figure 4.

During mass production, 797 PMT modules passed the quality controls for the assembly process.

3.4 Calibration of PMT modules

The gain and dark count level for qualified PMT modules were measured at the University of Science and Technology of China (USTC) laboratory. The measurement can be divided into three stages, a LED-based test, an evaluation with cosmic rays, and extra tests in preparation for outer space — such as vacuum heating and cooling, and mechanical vibration.

3.4.1 LED-based test system

To choose the proper PMT modules for each BGO bar, a LED-based system was set up to measure their gains and dark counts [14].

Figure 5(a) shows the configuration of the test dark box. It includes an integrating sphere with a LED light pulse fanned out through a bundle of 22 optical fibers, a front end electronics (FEE) board, a high-voltage (HV) fan-out board, and 22 grooves to place the PMT modules. These were coupled to a corresponding optical fiber coming from the integrating sphere. Because there are two dark boxes in our laboratory (figure 5(b)), 44 PMT modules can be tested at the same time and each test takes ~ 30 min.

After the PMT modules were placed in their position, the box was closed and locked. The LED was driven by a programmable pulse generator, and the light luminance increased gradually

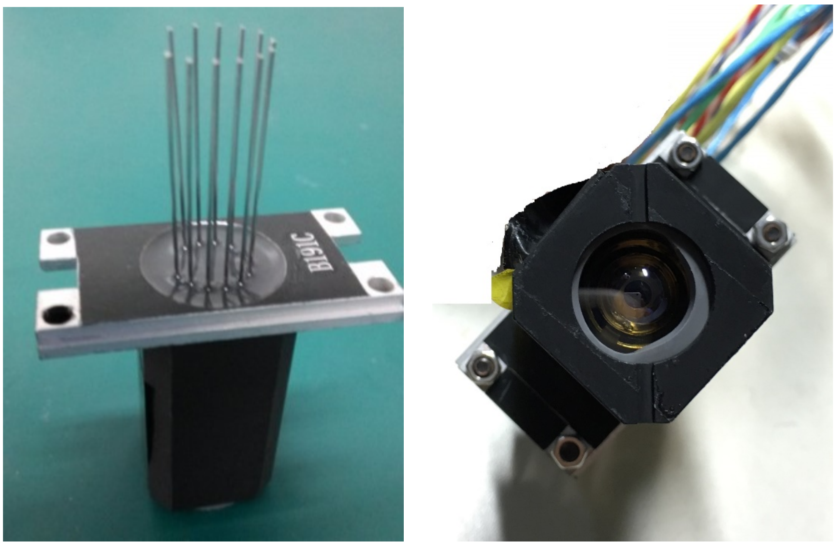

(a) (b)

Figure 3. (a) A PMT module after glue has been poured into the aluminum sleeve. (b) Glue blocking a part of the PMT faceplate. PMT modules like this were discarded.

by adjusting the output amplitude with Labwindows/CVI automatically [15]. Each PMT module was measured with a high voltage of 670 V. The outputs of dynodes 2, 5, and 8 from the 22 PMT modules to be tested were grouped and input to sample and hold VATA160 ASICs (previously VA32 ASICs) [16, 17] in the FEE board [6]. The trigger signal from the programmable generator was used to start the data acquisition (DAQ). The charge signals from dynodes 2, 5, and 8, from each of the 22 PMT modules, were digitized with a 16-bit ADC (AD976A, [18]) and the ADC counts recorded. The ADC counts measured from dynodes 2, 5, and 8 are referred to as DY2, DY5 and DY8 respectively for the rest of this document. Figure 6 shows a plot of the DY8 versus DY5, and DY5 versus DY2, for one of the PMT modules. A linear fit was carried out in each plot, from 500 counts to 700 counts in figure 6(a) and from 520 counts to 660 counts in figure 6(b) that is the region of operational interest for DAMPE. The gain from dynode 5 to dynode 8 is $\sim$ 45. The gain from dynode 2 to dynode 5 is $\sim$ 70. Thus the net gain of this PMT module is $\sim$ 3150. In addition, the reason for the saturation of dynode 8 and dynode 5 can be attributed to the limit of the input range of the VATA160 ASICs, in which the maximum range is $\sim$ 12 pC, and the corresponding ADC counts is $\sim$ 14000.

The distribution of gains for 797 PMT modules is shown in figure 7. The mean value of the gains between dynode 8 and dynode 5 is $\sim$ 60, while that between dynode 5 and dynode 2 is $\sim$ 65. To obtain the best gains, the PMT modules were required to have gains of 30–90 between dynode 2 and dynode 5, and between dynode 5 and dynode 8. 739 PMT modules passed these criteria.

The dynamic range (DR) of a PMT module can be defined as:

$$\mathrm{DR} = \mathrm{Ratio}_{8/5} \times \mathrm{Ratio}_{5/2} \,.$$

Figure 8 shows the DR distribution for the PMT modules. The DRs are all > 1000, which meet the requirements for DAMPE.

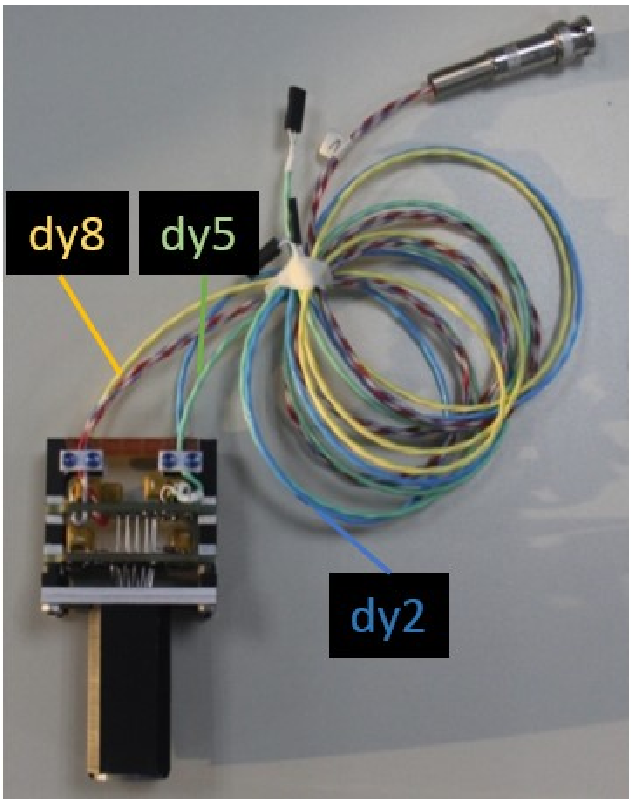

Figure 4. Photograph of the finished PMT module with baseboard assembled, where the multi-colored cable is the high voltage cable, and the blue, green and yellow cables are the signal cables for dynodes 2, 5 and 8 respectively.

The PMT module dark counts were measured using the LED test box, but without the LEDs being fired. The dark count rate is an important factor in determining the detection ability of a weak optical signal in a PMT module, so testing the PMT module for dark counts is crucial. Figure 9 shows the distribution of the dark-counts of 797 PMT modules measured in the LED-based system. They are all tested under a high voltage of 950V, which is a little higher than that used in space. PMT modules whose dark-count rates are $< 4\,\mathrm{Hz}$ were chosen for the DAMPE project. A total of 755 PMT modules passed this qualification.

711 PMT modules passed the quality controls in the LED-based test system. Thus over 88% of all PMT modules were found to be of high-performance, and passed the rigorous screening needed for DAMPE.

3.4.2 Cosmic ray test system

After the LED tests, the qualified PMT modules were sorted according to the gains between dynode 5 and dynode 8, and matched to particular BGO bars. The bars and modules were placed in a configuration representing the final arrangement in DAMPE, as shown in figure 10 [19]. When a cosmic ray muon passes through the detector, the output signals of the PMT modules are read out by the same electronics system as that used in the LED-based test stand.

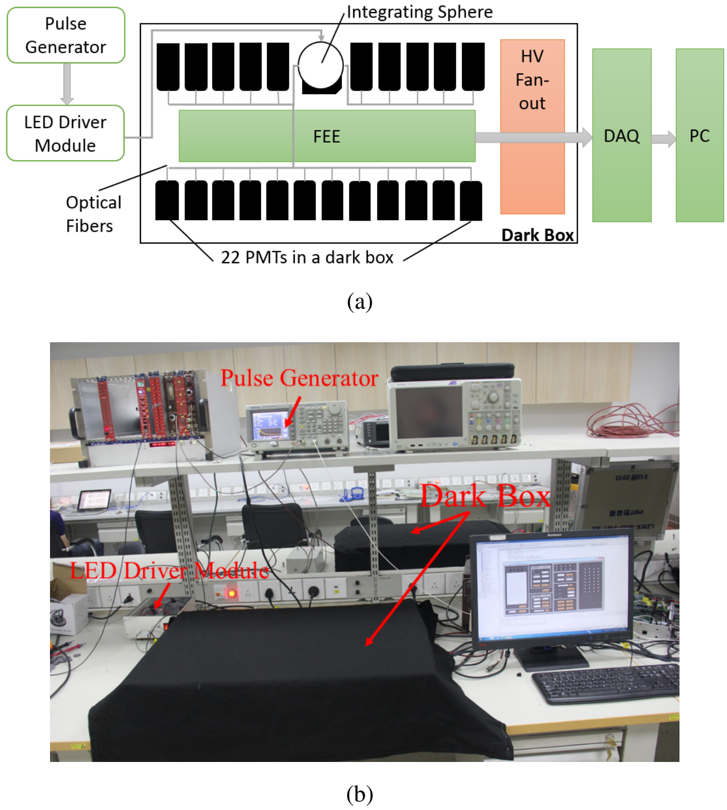

Figure 5. (a) Configuration in the dark box. (b) Photograph of the LED-based test system in our laboratory, which contains two dark boxes.

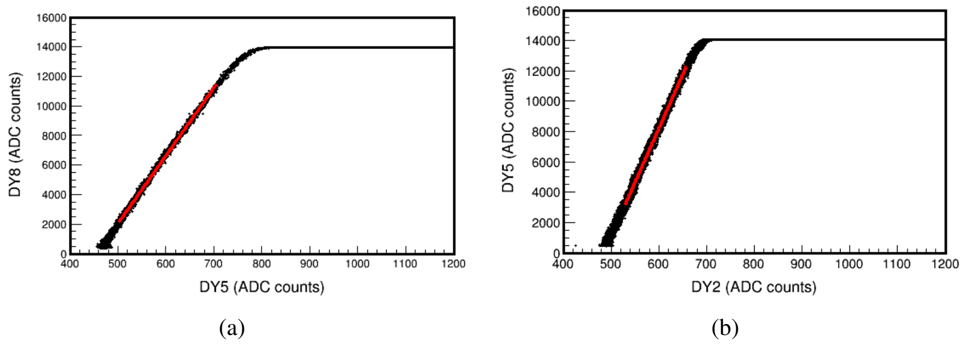

Figure 6. A typical plot of DY8 versus DY5 (a), and DY5 versus DY2 (b), for a PMT module. Also shown are the linear fits to the data in each of the two plots.

According to the cosmic-muon test, all the PMT modules performed well with their corresponding BGO bars. A typical distribution of the deposited energy from MIPs is shown in figure 11, from dynode 8 of a PMT module. The PMT modules and BGO bars performed well in the ground based cosmic ray test stand.

In the ground test, the deposited energies in each BGO bar are insufficient for making a visible dynode 2 signal from cosmic ray muons. Therefore, just the gains between dynode 5 and dynode 8

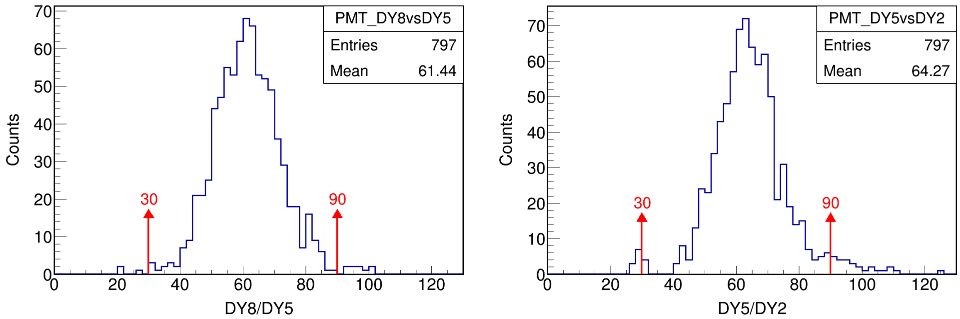

(a) (b)

Figure 7. Distribution of PMT module gains for dynode 5 to dynode 8 (a), and for dynode 2 to dynode 5 (b).

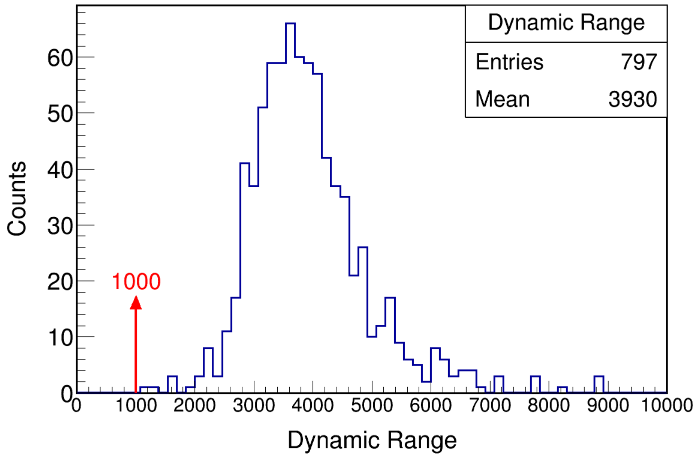

Figure 8. Distribution of PMT module DRs.

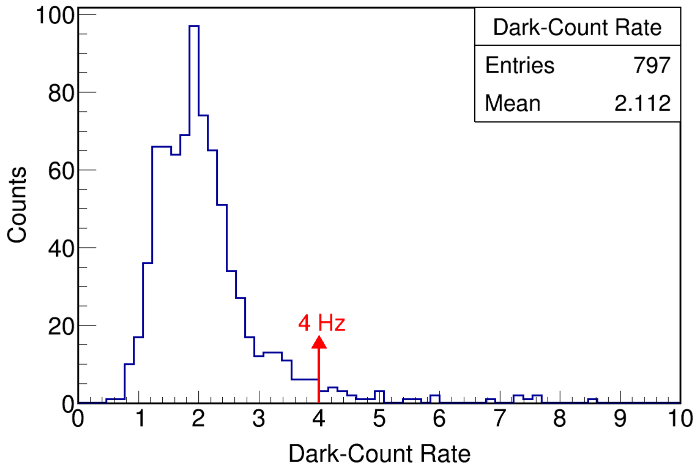

Figure 9. Distribution of the PMT module dark-count rates within 9 Hz.

were measured and analyzed. A typical correlation plot between dynode 5 and dynode 8 is shown in figure 12(a) from the cosmic-ray test stand. The distribution of gains between dynode 5 and dynode 8 in figure 12(b) is consistent with those in the LED-based test.

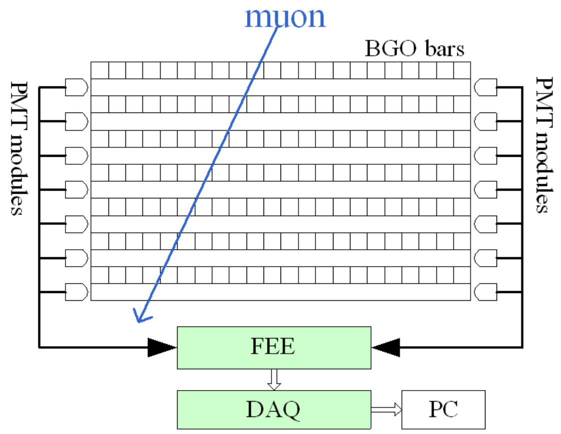

Figure 10. Configuration of the BGO bars and their corresponding PMT modules, in their final arrangement for DAMPE.

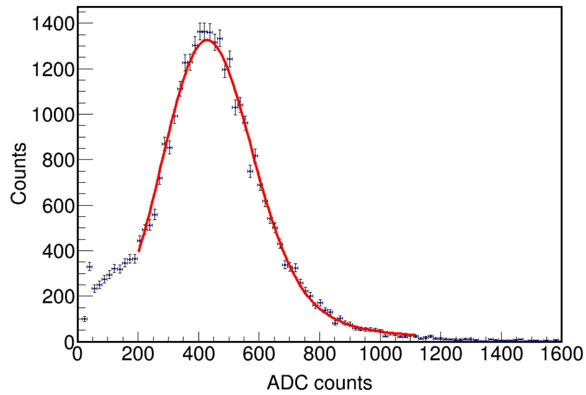

Figure 11. Typical distribution of signals from MIPs read out from dynode 8 of a PMT module.

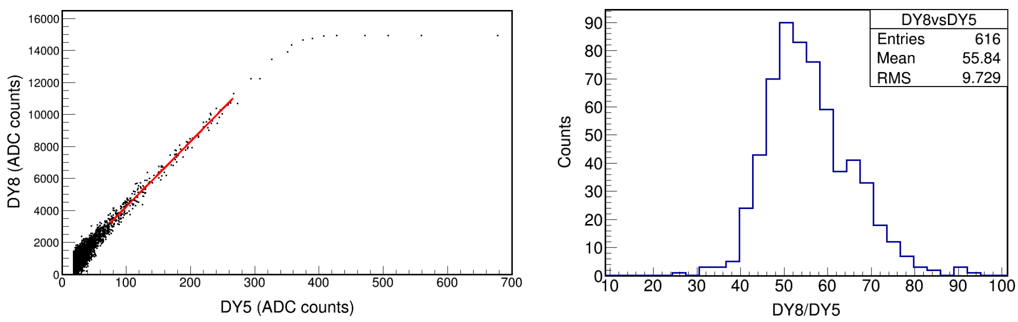

(a)

(b)

Figure 12. Typical plot of the correlation of outputs between dynode 5 and dynode 8 for a PMT module (a), and (b) the distribution of the gains between dynode 5 and dynode 8, from the cosmic ray test stand. The saturation of dynode 8 is caused by the limit of the input range of the VATA160 ASICs.

3.4.3 The examinations under extra space conditions

To test the performance of the PMT modules and their corresponding BGO bars for the conditions expected during launch, and in space, a set of examinations under extra "space conditions" was

2017 JINST 12 T05004

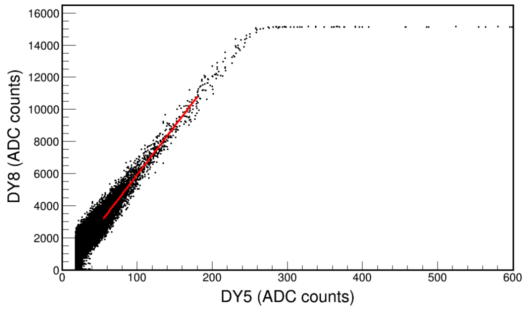

(a)

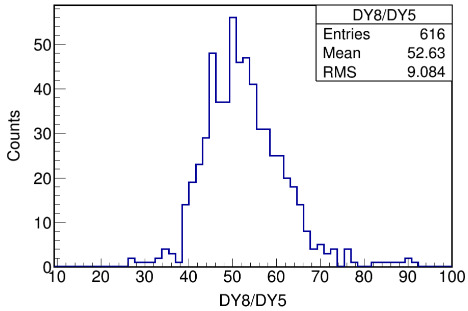

(b)

Figure 13. Typical plot of the correlation of outputs between dynode 5 and dynode 8 for a PMT module (a), and (b) the distribution of the gains between dynode 5 and dynode 8, after the extra space conditions. The saturation of dynode 8 is caused by the limit of the input range of the VATA160 ASICs.

developed (i.e., a vacuum heating and cooling test and a mechanical vibration test).

In the vacuum heating and cooling test, the final BGO ECAL was placed under vacuum, and 12.5 thermal cycling tests (−20 °C–+35 °C) were conducted to verify the thermal design of the detector [20]. During the mechanical vibration test, the detector was fixed onto a shaking platform, whose vibrations simulated the extreme cases of high vibration during launch. Sinusoidal vibration and random vibration tests with different levels were carried out according to the DAMPE Environmental Test Requirements for Payload and the User Manual for LM-2D. The detailed situation is described in [21].

After the examinations under extra space conditions, all of the PMT modules and the corresponding BGO bars performed well, which proves the efficacy of the selections of the 616 PMT modules. The system was measured in the cosmic-muon test stand. A typical plot of dynode 5 versus dynode 8 is shown in figure 13(a). The distribution of the gains between dynode 5 and dynode 8 is shown in figure 13(b), and are very similar to those from the initial cosmic test stand.

3.4.4 Verification in space

In space, MIPs were selected and used to calibrate PMT module gains from dynode 5 to dynode 8. Showering events were used to test PMT module gains from dynode 2 to dynode 5. Figure 14 shows the data from the calibration of a PMT module in space, with (a) the signals from dynode 5 versus dynode 8, and (b) from dynode 2 versus dynode 5.

As shown in figure 15, the distribution of gains measured in space is almost the same as those measured in the cosmic test on the ground. The PMT modules that passed all the quality controls on the ground were found to perform to the same level in space. The gains measured on the ground agreed with those measured in space to within 40%. Therefore, the tests on the ground have been extremely useful for the selection of the PMT modules for DAMPE and the characterization of their performance.

4 Conclusion

PMT modules, with high dynamic range readout, were installed in DAMPE to measure high energy electrons, positrons and gamma rays with energies from 5 GeV to 10 TeV. Quality control of mass

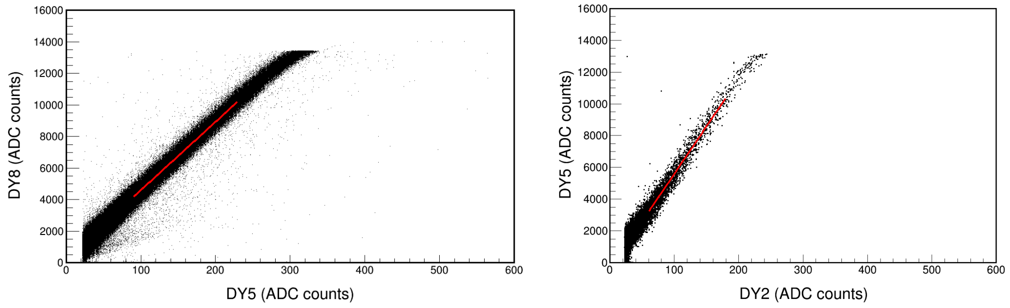

(a) (b)

Figure 14. Typical plots of the correlation of outputs between (a) dynode 8 and dynode 5 and (b) dynode 5 and dynode 2 from the space data.

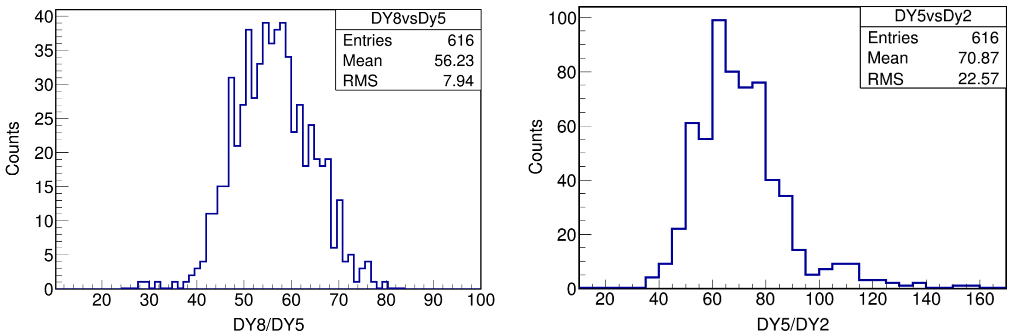

(a) (b)

Figure 15. Distributions of gains (a) between dynode 5 and dynode 8 and (b) dynode 2 and dynode 5 from the space data.

production PMT modules was performed. All the PMT modules were measured in detail on the ground. Over 88% of the PMT modules meet the requirements of DAMPE.

As a result, 616 qualified PMT modules were installed in the BGO ECAL and these all performed well in the ground experiment. The test results were stored in a database and were used as the calibration values for when the satellite is deployed in space. Comparing the test results from the ground and from space confirms that all the PMT modules work well in space, with the results in space, for the dynode gains, agreeing with those on the ground to within 40%. The successful operation of all the PMT modules in space is a reflection of all the important quality control and selection steps carried out on the ground.

Acknowledgments

This work was supported by the National Natural Science Foundation of China (Grant No. 11673021), the Strategic Priority Research Program on Space Science of Chinese Academy of Sciences (Grant No. XDA04040202-4), and the National Basic Research Program (973Program) of China (Grant No. 2010CB833002).

The authors are grateful to the colleagues in the DAMPE collaboration and the Shandong Institute of Aerospace Electronics Technology for their contributions to the PMT module production and tests.

2017 JINST 12 T05004

References

[1] J. Chang et al., *An excess of cosmic ray electrons at energies of* 300–800 *GeV*, *Nature* **456** (2008) 362.

[2] J. Chang, *Dark matter particle explorer: the first chinese cosmic ray and hard γ-ray detector in space*, *Chin. J. Space Sci.* **34** (2014) 550.

[3] Y. Li et al., *Testing the* 130 *GeV gamma-ray line with high energy resolution detectors*, *Phys. Lett.* **B 715** (2012) 35.

[4] J. Wu et al., *Dark progress of DAMPE: chinese high energy cosmic particle detector to be in space*, in the proceedings of the 33rd *International Cosmic Ray Conference*, July 2–9, Rio de Janeiro, Brasil (2013).

[5] Y. Zhang et al., *A high dynamic range readout unit for a calorimeter*, *Chin. Phys.* **C 36** (2012) 71.

[6] Feng C et al., *Design of the readout electronics for the BGO calorimeter of DAMPE mission*, *IEEE Trans. Nucl. Sci.* **62** (2015) 3117.

[7] Z. Zhang et al., *Design of a high dynamic range photomultiplier base board for the BGO ECAL of DAMPE*, *Nucl. Instrum. Meth.* **A 780** (2015) 21.

[8] Hamamatsu, *R5610A Photomultiplier tube*, https://www.hamamatsu.com/us/en/R5610A.html.

[9] R. Boll et al., *Applications of amorphous magnetic materials in electronics*, *IEEE Trans. Magneti.* **17** (1981) 3053.

[10] D. Corning, *Sylgard 170 fast cure silicone elastomer kit*, http://www.dowcorning.com/applications/search/default.aspx?R=282EN.

[11] Quality management system for the aerospace industry, AS9100, http://standards.sae.org/as9100c/.

[12] J.H.L. Pang et al., *Thermal cycling analysis of flip-chip solder joint reliability*, *IEEE Trans. Comp. Pack. Technol.* **24** (2001) 705.

[13] GD414, a silicon rubber made in China, used in the aerospace industry, see webpage.

[14] J. Dong et al., *Development of an automatic test system for the PMTs used in the BGO ECAL of DAMPE*, PoS(ICRC2015)1195.

[15] T. Xiang et al., *Study of linearity for a high dynamic range calorimeter*, *Chin. Phys.* **C 38** (2014) 046201.

[16] IDEAS, *33 channel high-dynamic range CSA with sample-and-hold*, http://www.ideas.no/products/va32hdr14-3/.

[17] S. Gao et al., *The radiation tolerance studies on the VA32 ASIC for DAMPE BGO calorimeter*, *Nucl. sci. Tehcn.* **25** (2014) 010402.

[18] Analog Devices, *AD976A: a high speed, low power 16-bit A/D converter*, http://www.pci-card.com/AD976.pdf

[19] Z. Zhang et al., *The calibration and electron energy reconstruction of the BGO ECAL of the DAMPE detector*, *Nucl. Instrum. Meth.* **A 836** (2016) 98.

[20] Y. Wei et al., *Temperature dependence calibration and correction of the DAMPE BGO electromagnetic calorimeter*, 2016 *JINST* **11** T07003.

[21] Y. Hu et al., *Environmental test of the BGO calorimeter for dark matter particle explorer*, *Chin. Phys.* **C 40** (2016) 11.

2017 JINST 12 T05004